Hindawi
Shock and Vibration
Volume 2017, Article ID 3638150, 9 pages
https://doi.org/10.1155/2017/3638150

Research Article

Experimental Study of Bilinear Initiating System Based on Hard Rock Pile Blasting

Yusong Miao,[1] Xiaojie Li,[1] HongHao Yan,[1] Xiaohong Wang,[1] and Junpeng Sun[2]

[1]*Department of Engineering Mechanics, Dalian University of Technology, Dalian, Liaoning 116024, China*
[2]*Dalian Economic Development Zone Jinyuan Blasting Co., Ltd., Dalian, Liaoning 116600, China*

Correspondence should be addressed to Xiaojie Li; samuelstone@126.com

Received 22 March 2017; Revised 25 June 2017; Accepted 7 August 2017; Published 1 October 2017

Academic Editor: Onome E. Scott-Emuakpor

It is difficult to use industrial explosives to excavate hard rock and achieve suitable blasting effect due to the low energy utilization rate resulting in large rocks and short blasting footage. Thus, improving the utilization ratio of the explosive energy is important. In this study, a novel bilinear initiation system based on hard rock blasting was proposed to improve the blasting effects. Furthermore, on the basis of the detonation wave collision theory, frontal collision, oblique reflection, and Mach reflection during detonation wave propagation were studied. The results show that the maximum detonation pressure at the Mach reflection point where the incident angle is 46.9° is three times larger than the value of the explosive complete detonation. Then, in order to analyze the crack propagation in different initiation forms, a rock fracture test slot was designed, and the results show that bilinear initiating system can change the energy distribution of explosives. Finally, field experiment was implemented at the hard rock pile blasting engineering, and experimental results show that the present system possesses high explosive energy utilization ratio and low rock fragments size. The results of this study can be used to improve the efficiency in hard rock blasting.

1. Introduction

Given that the mechanical technology has not fully matured, drilling-and-blasting is still the preferred method for hard rock excavation. Blasting footage and moderate rock fragmentation size play important roles in the excavation cycle, and these operations are a major cost of an excavation project [1, 2]. Accordingly, the safety, efficiency, and economics of hard rock blasting are the problems that should be solved immediately. Several studies have been conducted on two methods of hard rock blasting [3–5]. The first method is rock and explosive performance matching [6]. Three matching theories exist, namely, energy matching, whole processing matching, and acoustic impedance matching. Energy matching theory considers that explosive energy can adapt to the hard rock break energy by increasing or decreasing the explosive charge. Whole processing matching theory only considers the interaction energy between the explosive and the hard rock in the entire blasting process. However, accomplishing a complete coupling detonation wave is impossible even when the boreholes are completely filled with explosives [7]. Acoustic impedance matching theory is based on the incident and reflected effect on a rock interface, and the energy efficiency is considered the highest when the acoustic impedances of the explosive and the hard rock are equal. According to the acoustic impedance computational formula [8], when the rock acoustic impedance value is 1.33×10^4 kg/(m^2·s) (i.e., the density and detonation velocity are 2.83×10^3 kg/m^3 and 4,700 m/s, resp.), the acoustic impedance of No. 2 rock emulsion explosive value should be 5.45×10^3 kg/(m^2·s) (i.e., the density and detonation velocity are approximately 1.14×10^3 kg/m^3 and 4,780 m/s, resp.) to obtain the acoustic impedance matching. Thus, the two aspects of explosive density and detonation velocity should be explored. However, both aspects have limits that if exceeded, the explosives cannot explode steadily. Therefore, the satisfaction of blasting requirements is difficult through acoustic impedance matching, and enhancing the utilization rate of explosive energy is an effective approach for improving the blasting effects.

The shaped charge, notched blasting, and multipoint initiating technology should also be considered. Under the special conditions, the shaped charge can focus the effect of explosion energy by a hollow or void cut on the explosive surface [9]. Different shaped charges, such as linear, conical, and spherical, have been used for cutting, demolition, penetrating armor, and forming metal. Lots of the shaped charge devices consist of a metal liner on the charge cavity. They can cut hard objects to a depth seven times deeper or more than the conventional blasting. These devices have been widely used in the field of civil blast engineering [10, 11]. Chen et al. [12] invented a new type of jet cracker to improve the blasting efficiency and the length of cyclical footage. However, when the shaped charge is applied to the hard rock blasting, two disadvantages are observed. First, the integrity of the hollow or void cut must be guaranteed. Once the boreholes are filled with water or other debris, it will not be able to attain the expected effect of the shaped charge. Second, the explosive loading decreases because the charge cavity occupies the borehole space to lower the borehole utilization, which makes the shaped charge difficult to apply in engineering blasting. Notched blasting is also a method of preformed cracks after borehole drill is completed according to the theory of fracture mechanics; this method can improve the blasting effect and decrease the charge, the cutting angle, the direction, and the depth, which are the important factors to determine notched blasting effect [13, 14]. Yue et al. [15] utilized the digital lased dynamic caustics system to study the crack propagation velocity and dynamic stress intensity of notched and non-notched borehole cut blasting. Zheng et al. [16] optimized the periphery borehole charge and charge structure to improve the efficiency of traditional cutting blasting. Rathore and Bhandari [17] adopted different types of liner notching inside the borehole to determine the rock damage and studied the damage quantification in single circular and notched holes. This method is mainly used in presplitting or smooth blasting and is difficult to apply in engineering blasting because of the complex drilling process. Furthermore, multipoint initiating technology based on the detonation wave collision is a new type of warhead control, which can decrease the reaction time of the charge and increase the energy utilization of the explosive [18]. This method is mainly applied in military fields, such as explosively formed penetrators (EFP) [19], linear EFP [20], and ammunition design [21]. Satisfactory results in engineering blasting are also rarely obtained because delay time of industrial detonators is in the microsecond magnitude; thus, a simultaneous initiation is difficult to guarantee [22].

Given the above-mentioned analyses, there is a pressing need to determine a novel and efficient method for hard rock engineering blasting. The current study investigated the explosion effects of the bilinear initiating system, a symmetrical arrangement of the two detonating cords on the sides of a cartridge to increase the detonation wave pressure, through physical simulations and field experiments. The applied technology analysis and result comparison show that the proposed system is efficient for hard rock blasting, which avoids the complicated processes of shaped charge, lowers the blasting cost, and improves the working efficiency.

2. Detonation Wave Collision Theory

Detonation wave collision is a common problem in multipoint initiation technology; this is because the collision and convergence of the detonation wave can change the waveform and increase the pressure of the detonation wavefront [23]. At first, the plane detonation wave propagation, collision, oblique reflection, and Mach reflection in the borehole were analyzed to describe the entire process of detonation wave collision. After the initiation of the explosive at two symmetric initiation points (Figure 1), two spherical detonation waves are propagated independently in the borehole at the same velocity and strength, which are shown as the reflection of a detonation wave on the rigid wall. Frontal collision occurs when the two detonation waves reach the centerline and the pressure at the point of the collision increases sharply. The detonation wave is transmitted along the centerline and collides to form oblique reflection, with the pressure increasing. Mach reflection subsequently occurs when the incidence angle reaches a certain value, which has a higher pressure and larger increase in the energy density and temperature [24, 25]. The entire process was analyzed as follows based on the theory of detonation shock dynamics.

The explosive detonation process from the initiation to the completion is completed in an instant. Chapman-Jouguet (C-J) theory [26] states that the detonation in the explosive detonation process is assumed to be ideal, in which the energy is released instantaneously and perfectly confined. In the detonation wave propagation zone shown in Figure 1, the parameters of the complete explosive detonation can be calculated with the following equations:

$$\begin{aligned} p_H &= \frac{1}{\gamma+1}\rho_0 D^2; \\ v_H &= \frac{\gamma}{\gamma+1}v_0; \\ \rho_H &= \frac{\gamma+1}{\gamma}\rho_0, \end{aligned} \tag{1}$$

where p_H is the pressure of the explosive complete detonation, ρ_0 and ρ_H are the initial and complete detonation explosive density, respectively, D is the velocity of the detonation, v_H is the particle velocity of the detonation products, and γ is the exponent in the polytropic equation of state, which can be calculated from ρ_0 [27]:

$$\gamma = \frac{\left(1.01 + 1.313\rho_0\right)^2}{1.558\rho_0} - 1. \tag{2}$$

The frontal collision zone of Figure 1 shows that the normal reflection occurs after the detonation wave has collided. Given the conservations of mass, momentum, and energy, p_1/p_H can be expressed as follows:

$$\frac{p_1}{p_H} = \frac{5\gamma + 1 + \sqrt{17\gamma^2 + 2\gamma + 1}}{4\gamma}. \tag{3}$$

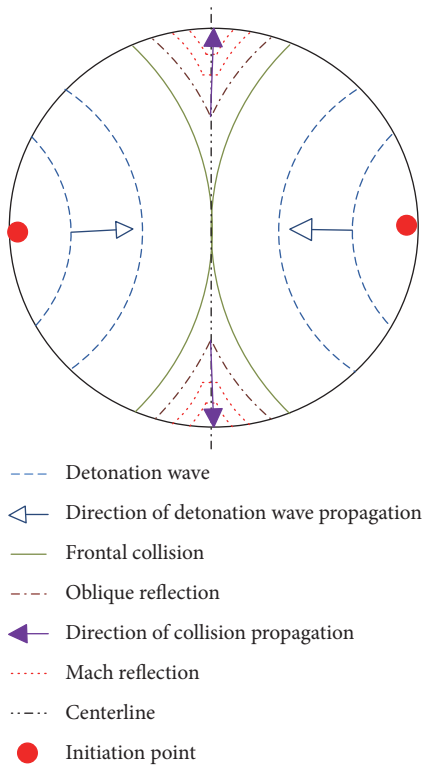

Figure 1: Entire process of detonation wave propagation.

The detonation wave propagation is in the form of a regular oblique reflection wave as shown in the oblique reflection of Figure 1.

Figure 2 shows the oblique reflection configuration. The known parameters of the former reflection wave OR are p_H, ρ_H, and q_1, and those of the latter reflection wave OR are p_2, ρ_2, and q_2. Furthermore, the set up u_{1n} and u_{2n} are the components of the perpendicular to the OR wave surface. Given the geometric relationships shown in Figure 2, the following equations are valid:

$$\frac{\tan(\phi-\theta)}{\tan\phi}=\frac{(D-u_H)/v_1}{D/v_0}=\frac{\gamma}{\gamma+1}, \tag{4}$$

where θ are the normal and tangential components of the deflection angle from its original direction and ϕ is the incidence angle. Furthermore, the following expression of the deflection angle θ is provided through (4):

$$\theta=\arctan\left(\frac{\tan\phi}{\gamma\tan^2\phi+\gamma+1}\right). \tag{5}$$

According to the conservation of mass and momentum, the following equations are valid:

$$\begin{aligned}\rho_H u_{1n}&=\rho_2 u_{2n},\\ p_H+\rho_H u_{1n}^2&=p_2+\rho_2 u_{2n}^2.\end{aligned} \tag{6}$$

Substituting the detonation state equation $p=A\rho^k$ [18] into (1), then (6) can be expressed as follows:

$$\frac{\rho_H}{\rho_2}=\frac{v_2}{v_H}=\frac{(\gamma-1)p_2+(\gamma+1)p_H}{(\gamma+1)p_2+(\gamma-1)p_H}. \tag{7}$$

From the geometric relationships shown in Figure 2, we can determine the following equation:

$$\frac{\tan(\varphi+\theta)}{\tan\varphi}=\frac{(\gamma+1)p_2+(\gamma-1)p_H}{(\gamma-1)p_2+(\gamma+1)p_H}. \tag{8}$$

The pressure p_2 of the detonation oblique reflection in (8) can be calculated as follows:

$$\frac{p_2}{p_H}=\frac{(\gamma+1)\tan(\phi+\theta)-(\gamma-1)\tan\phi}{(\gamma+1)\tan\phi-(\gamma-1)\tan(\phi+\theta)}, \tag{9}$$

where γ can be calculated from ρ_0 for a given incidence angle ϕ by using (2). Given that p_2/p_H is a function of ϕ, θ, and γ in (9), they can be calculated in accordance with the following equations:

$$\begin{aligned}p_H&=\frac{\rho_0 D^2}{\gamma+1}=\frac{\gamma}{(\gamma+1)^2}\rho_H D,\\ q_1^2&=D^2\left[\left(\frac{\gamma}{\gamma+1}\right)^2+\cot^2\varphi\right],\\ \theta&=\arctan\left(\frac{\tan\phi}{\gamma\tan^2\phi+\gamma+1}\right).\end{aligned} \tag{10}$$

The relationship between the angle of incidence ϕ and reflection angle φ can be solved from (9) to (10) as follows:

$$\begin{aligned}\frac{\tan\varphi}{\tan(\varphi+\arctan(\tan\phi/(\gamma\tan^2\phi+\gamma+1)))}&=\frac{(\gamma-1)}{\gamma+1}+\frac{2\gamma^2}{\gamma+1}\\ &\cdot\frac{1}{\left[\gamma^2+(\gamma+1)^2\cdot\cot^2\phi\right]\cdot\sin^2(\varphi+\arctan(\tan\phi/(\gamma\tan^2\phi+\gamma+1)))}.\end{aligned} \tag{11}$$

The reflected angle is an imaginary solution when the incident angle reaches 46.9° through (11). The reflected shock can catch the incident shock, and a single merged shock is formed in the Mach reflection zone of Figure 1. This phenomenon is called Mach reflection, and the merged shock is called the Mach stem [28]. The point located at the incident,

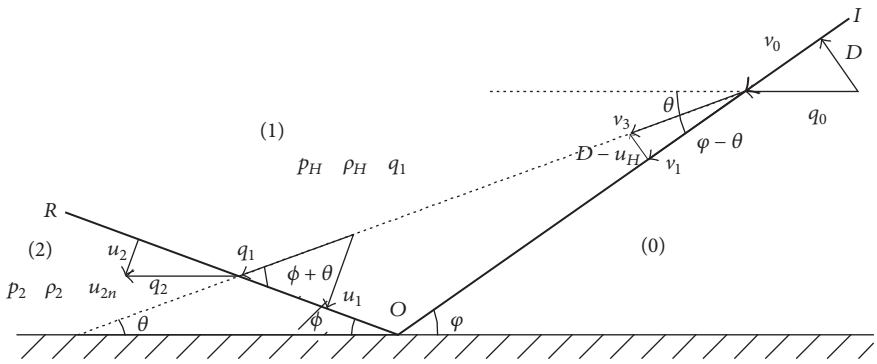

FIGURE 2: Detonation wave oblique reflection map in the coordinate system. (0), initial state; (1), stable detonation state; (2), oblique reflection state.

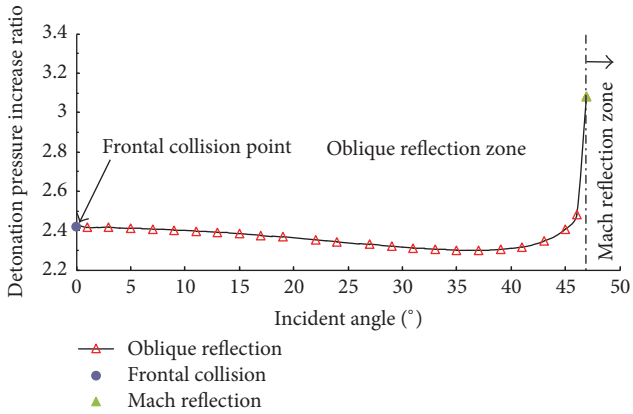

FIGURE 3: Relationship between the detonation pressure increase ratio and incident angle.

reflected, and Mach shocks intersect is called the triple point. The pressure p_3 of the Mach reflection can be calculated as follows:

$$\frac{p_3}{p_H} = \frac{1}{\sin^2\phi} + \frac{1}{\sin\phi}\left(\frac{1}{\sin^2\phi} - \frac{Q_3}{Q}\right)^{1/2}, \quad (12)$$

where Q is the chemical energy of the C-J detonation reaction and Q_3 is the chemical energy of the Mach reaction.

Figure 3 shows the relationship between the ratio of the detonation pressure and incident angle in the bilinear initiating system. At the incident angle $\phi = 0^\circ$, the frontal collision occurs, and the rate of pressure increase is 2.41-fold. As the incident angle increases, the oblique reflection occurs and the pressure increasing ratio varies from 2.3 to 2.47 where the incident angle is between 0° and 46.9°. The pressure increasing ratio sharply jumps to 3.08 with the occurrence of the Mach reflection, where $Q_3 = Q$ is assumed.

3. Simulation Experiment

A bilinear initiating system is applied in engineering blasting to realize the increasing pressure of the detonation wave collision. Combined with the previous theoretical analyses, the current authors designed a series of blasting experiments [29], such as the explosive-determination of power and brisance test. The results show that the bilinear initiating system can change the detonation pressure distribution in a particular direction and the detonation wave collision can improve the utilization ratio of explosive energy. However, the boreholes are besieged by the rock in actual engineering blasting; the standard tests are too simple to show the blasting effects of rock. Observing and analyzing the rock fracture and fragmentation processes around the boreholes are also difficult as demonstrated in the field experiments [30, 31].

Therefore, a model was built consisting of steel plates, rubber plates, and a test plate as shown in Figure 4 to simulate the different crushing effects under the bilinear and detonator initiating system. First, 500 mm × 500 mm steel plates were cut and employed as the base and cover plates. Second, a piece of 300 mm × 300 mm steel was cut and adopted as the pressing plate, and a granite plate was utilized as the test plate. Third, 300 mm × 300 mm rubber plates were cut and used as the buffer cushions to avoid the interactions between the steel and granite plates. The base plate was connected to the cover plate by reserving eight M-16 bolt holes. Finally, 20 mm diameter holes were drilled into the cover plate, the pressing plate, the buffer cushion, and the test plate.

The model was placed on a flat ground prior to the start of this experiment. A layer of the buffer cushion was tiled in the trough. A test plate was then placed on top of the buffer cushion. Another layer of the buffer cushion was tiled on top of the test plate, and the pressing plate was placed in the second layer of the buffer cushion. Finally, the bolts were tightened, and covering was applied to the model.

Two types of initiating methods were designed. The first type is the detonator initiating system (Figure 4), wherein the Nonel ignites the detonator or initiating charge, which then sets off the main charge. The other type is the bilinear initiating system, which has two detonating cords as the initiating body arranged symmetrically on both sides of the borehole. The delay detonator ignites the detonating cord and then detonates the main charge.

Dye penetrant inspection (DPI) was used after the cover plate was taken off after blasting to inspect and analyze the cracks within the rock. Figure 5 shows the results of the simulated experiment. The fracture area in the bilinear initiating

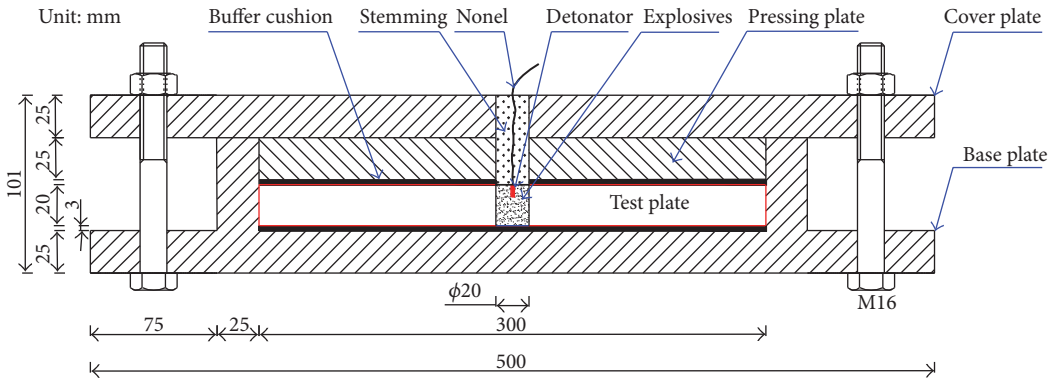

Figure 4: Schematic of the physical model.

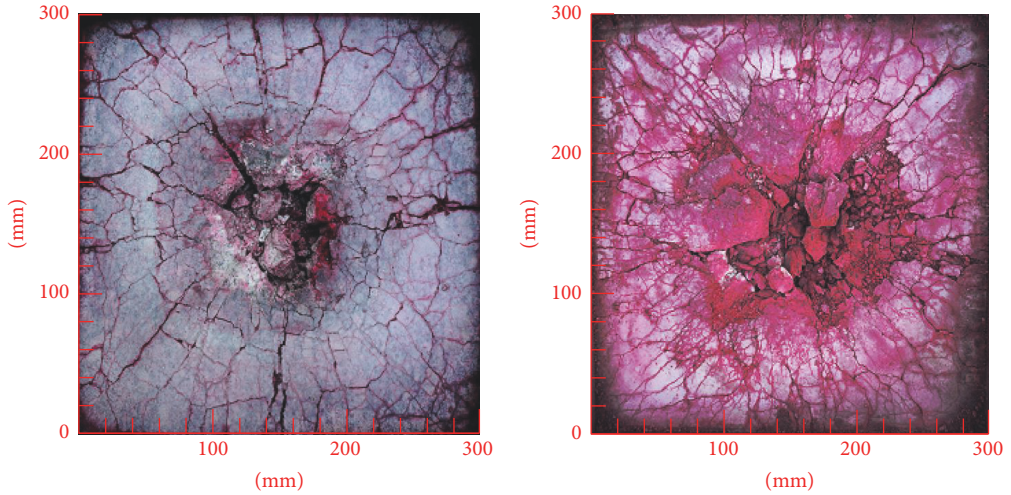

(a) Detonator initiating system

(b) Bilinear initiating system

Figure 5: Results of the simulated experiment.

system is unevenly spread outward along the borehole, and the area is 288.59 cm^2, which is 1.10 times larger than that in the detonator initiating system. Furthermore, the maximum crack length is 1.44 times longer than that by the detonator initiating system.

With the application of the MATLAB development platform, watershed segmentation and Mayer's flooding algorithm were implemented to determine the crack widths and the corresponding ratios. Watershed segmentation is a transformation on the basis of a gray scale image. Mayer's flooding algorithm also works on the gray scale images. Watershed fragmentation with an adjacent catchment basin was constructed when the pixels on the gray scale were shown. The entire process includes the image gray scale processing (to enhance the contrast of the image), smooth filtering (to eliminate noisy point), gradient processing (to realize the grading of gray scale from low to high in the crack edge), edge detection, and watershed segmentation.

As shown in Figure 6, the ratios of the 3-4 mm crack widths of the bilinear initiating system are 39% and 37.5%, respectively, and the largest crack width is 12 mm. For the

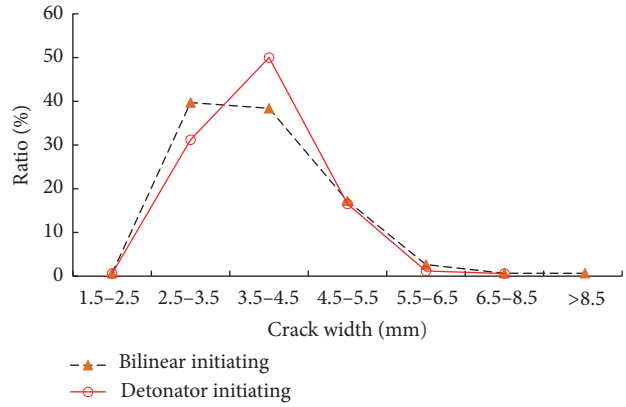

Figure 6: Ratios of crack widths from the physically simulated experiment.

detonator initiating system, nearly 50% of the crack widths are within 3.5–4.5 mm and the largest crack width is 8 mm. The total number of cracks (373 branches) produced by the

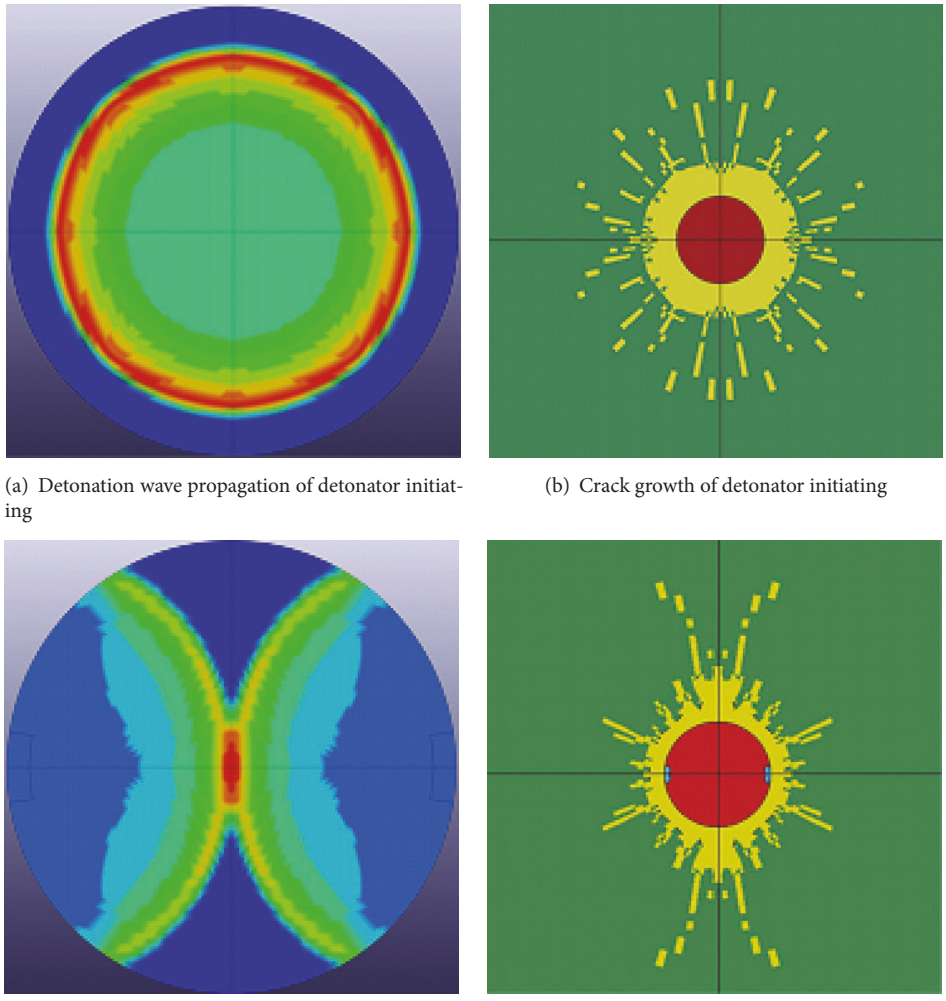

(a) Detonation wave propagation of detonator initiating

(b) Crack growth of detonator initiating

(c) Detonation wave propagation of bilinear initiating

(d) Crack growth of bilinear initiating

Figure 7: Detonation wave propagation and crack growth under two different initiating forms.

bilinear initiating system is larger than that by the detonator initiating system. The principle of conservation of energy [32] states that the higher the amount of energy used to produce cracks, the better the rock breakage.

Otherwise, fluid-solid coupling algorithm in the LS-DYNA^{3}d was applied to analyze the propagation of detonation wave and the process of rock fracture for the above two cases. The Jones-Wilkins-Lee (JWL) equation of states (EOS) was suited for modeling the pressure generated by the expansion of the explosive detonation product, and rock adopted the build-in bilinear kinematic hardening model (*MAT_ PLASTIC KINEMATIC) of program. As shown in Figure 7, when detonator initiating is used, the detonation wave starts uniformly from the initiation point and extends toward the edges, and the fissures also diffuse evenly. While, using the bilinear initiating system, it starts to spread from the symmetric boreholes initially, collision occurs at the centerline; and the maximum detonation pressure of the centerline is at least twice that of the former; and the large diameter crack will initially be generated at the centerline and then expand outwards. It also indicates that bilinear initiating system can change the explosive's energy distribution on rocks.

4. Field Experiment of Bilinear Initiating System

4.1. Site Description. The construction of Haiwan Square, which is located in the Economic and Technological Development Zone of Dalian, was selected for the field experiment in this study. The building includes office, resident quarters, a supermarket, and a car park. The construction period was relatively short; thus, the period for the foundation pit excavation was limited. The rock properties in the foundation are granite density (2,830 kg/m^3), Poisson's ratio (0.27), compression strength (145.7 MPa), shear strength (20 MPa), tensile strength (4.6 MPa), elastic modulus (57 GPa), and cohesion (25 MPa).

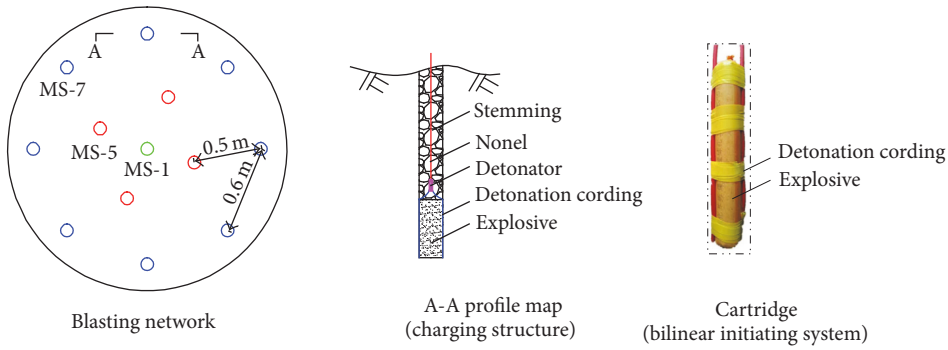

Figure 8: Blasting network and cartridge.

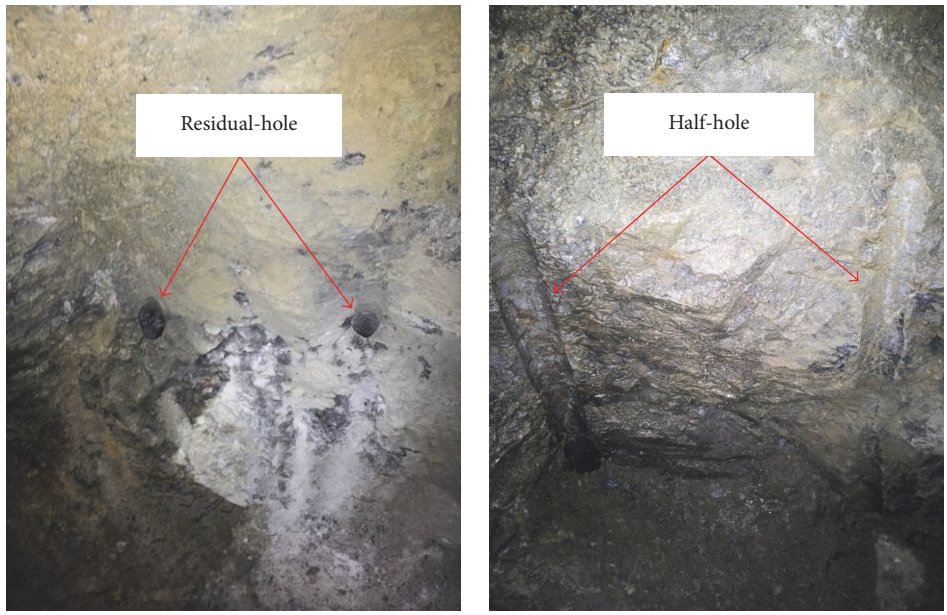

(a) Results of detonator initiating blasting (b) Results of bilinear initiating blasting

Figure 9: Blasting footage and half-hole of the field experiment.

4.2. Blast Parameters Design. The blasting parameters were calculated on the basis of the theoretical analysis, simulation experiment in Section 3, and related calculation method of pit excavation blasting. The depth and diameter of each borehole are 0.8 m and 42 mm, respectively. The spacing and burdening of the boreholes are 0.6 and 0.5 m, respectively. The boreholes were drilled with the Y-26 portable rock drill. Each hole was charged with a maximum of 0.3 kg No. 2 rock emulsion explosive because of the requirement of blasting vibration for the surrounding buildings.

The borehole patterns for the pile blasting and charging structure are shown in Figure 8. The detonator initiating system (conventional blasting operation) utilized No. 2 rock emulsion explosive as the main charge and a detonator as the initiation system with a staggered pattern. The bilinear initiating system also adopted the No. 2 rock emulsion explosive as the main charge. However, double symmetrical layout detonating cords were used as the initiation system as shown in Figure 8. The stemming, network connection, and other operation forms were set to be the same.

4.3. Results and Discussion. Blasting footage and rock fragmentation play vital roles in the efficiency and productivity of pile blasting. If the blasting footage and rock fragmentation are not controlled properly, they may increase the production cost and delay the excavation process because they may require a secondary drilling or crushing. Therefore, the blasting footage and the rock fragmentation are the main factors to evaluate the blasting effect. The blasting rock size in this excavation project was limited to less than 6 cm. Once it surpasses the control size, a breaker or a crusher may be used in secondary crushing of the rock into a smaller size.

Figure 9(a) shows the footage and half-hole of the detonator initiation system. Practically no breakage effect and half-hole are observed, and the peripheral contour of the pile is rough. The breakage efficiency is extremely poor, the footage

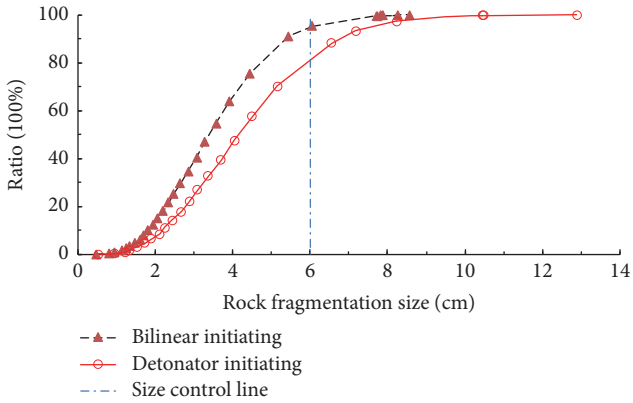

FIGURE 10: Rock fragmentation size of the field experiment.

is only 0.35 m, and the residual-hole still exists after blasting. Figure 9(b) shows that when using the bilinear initiating system, the half-hole ratio reaches 96%, the breakage effect is excellent, and the footage reaches 0.7 m, which is nearly twice that of the former. The quality of the periphery contour is improved after the blasting, and the damage to the surrounding rock significantly decreases. The results show that the bilinear initiating system effectively uses the explosive energy. The reason for such high utilization ratio is explained as follows. When the explosive is detonated by detonating cords, the detonating wave propagated and collided at the centerline. The formation of an uneven detonation pressure surface led to a damage fracture, which forms much blasting energy into the crack and accelerates the rock destruction.

The rock fragmentation of blasting can be measured through blasting muck pile photographs. The fragments in the photographs were compared with standard size objects, such as a ball with known diameter. The exercise attempts to determine the object that matches the fragment in terms of size and texture. The known scaling can be employed to deduce the rock fragmentation size in the blasting through the watershed segmentation technology.

Figure 10 shows the distribution curves of the rock fragmented size that resulted from the detonator and the bilinear initiating system. In the conventional detonator initiating system, approximately 80% of the rock fragmented sizes are less than the size control value of 6 cm, and the largest is 13 cm, wherein nearly 3% of the rocks with sizes larger than 9 cm must be secondarily crushed. This process increases the cost and has serious repercussions on the blasting excavation cycle. In the bilinear initiating system, approximately 92% of the fragmentation volume is less than 6 cm, and the largest is only 8.4 cm. Therefore, secondary crushing is unnecessary, and higher working efficiency is attained.

The current authors also applied the bilinear initiating system to the shield tunnel boulder blasting in No. 5 and No. 6 water intake tunnels of the Hongyan River Nuclear Power Station, Dalian, Liaoning Province, China. The drill stuck phenomenon occurs frequently, and the driving rate of the shield machine cannot reach the bedrock excavation rate when using the conventional detonator initiating system. Thus, the bilinear initiating system was adopted under the same blasting parameters. The field application results have shown that bilinear initiating system can lower the boulder strength, do without secondary crack and no blasting toe residual, and increase the shield tunneling speed by 42.7% than the conventional one. These conditions indicate that the bilinear initiating system can improve the energy efficiency of explosives and shorten the blasting excavation cycle time.

5. Conclusions

This study developed a novel bilinear initiating system. The cutting ability of the novel method was examined through theoretical analysis and physical simulation experiment. Field experiment was performed at the Economic and Technological Development Zone of Dalian, Liaoning Province, China. The primary conclusions are presented as follows.

The detonation wave propagation and collision process of the bilinear initiating system were analyzed based on the classical theory of detonation. The formula for calculating the detonation pressure of the frontal collision, oblique reflection, and Mach reflection was also derived. The results show that the detonation pressure of No. 2 rock emulsion explosive can be increased 2.41, 2.47, and 3.08 times, respectively.

A comparison of the physical simulation experimental results shows that the fracture area is larger and the rock fragmentation ratio of the bilinear initiating system is higher than that of the detonator initiating system. Furthermore, numerical simulation results also show that the bilinear initiating system can change the explosive's energy distribution and increase the utilization rate of explosive energy.

The theory and physical simulation experiment results were validated by the field experiment of the hard rock pile blasting and boulder blasting of tunneling excavation. The field data shows that the novel initiation method can decrease the size of rock fragments, improve the blasting footage, and lower the cost of secondary drilling or crushing. However, further optimization processes are necessary for more general applications, such as cut blasting and underwater blasting of hard rock with a strong clamp force.

Conflicts of Interest

The authors declare that they have no conflicts of interest.

Acknowledgments

This project is financially supported by the National Natural Science Foundation of China (nos. 11672067 and 11672068) and Dalian Jinyuan Blasting Co., Ltd., Liaoning Province, China. The authors wish to express their thanks to all of their sponsors.

References

[1] B. Sushil, *Engineering Rock Blasting Operations*, A. A. Balkema publishers, 1997.

[2] P. K. Singh, M. P. Roy, R. K. Paswan, M. Sarim, S. Kumar, and R. Ranjan Jha, "Rock fragmentation control in opencast blasting,"

Journal of Rock Mechanics and Geotechnical Engineering, vol. 8, no. 2, pp. 225–237, 2016.

[3] R. Long, S. Sun, Z. Lian, Y. Liao, and X. Qin, "A new technology for hard-rock tunneling based on drilling and hydraulic impact breaking," *International Journal of Mining Science and Technology*, vol. 25, no. 6, pp. 1053–1058, 2015.

[4] G. R. Tripathy and R. R. Shirke, "Underwater drilling and blasting for hard rock dredging in indian ports—a case study," *Aquatic Procedia, International Conference on Water Resources, Coastal and Ocean Engineering*, vol. 4, pp. 248–255, 2015.

[5] D. Karstens and H. Kuttruff, "Pressure histories during reflexion of electromagnetically driven shock waves in various gases," *Zeitschrift Fur Angewandte Physik*, vol. 28, no. 4, pp. 201–205, 1970.

[6] Z. D. Leng, W. B. Lu, P. Yan, M. Chen, and Y. G. Hu, "A new theory of rock-explosive matching in drilling and blasting based on reasonable control of the crushed zone," *Engineering*, vol. 12, no. 6, pp. 32–38, 2014.

[7] R. Nateghi, "Prediction of ground vibration level induced by blasting at different rock units," *International Journal of Rock Mechanics & Mining Sciences*, vol. 48, no. 6, pp. 899–908, 2011.

[8] S. S. Lu, *Research Dynamic Response and Failure Mode of Tunnel Surrounding Rock under Blasting Loading*, Tianjing University, 2012.

[9] W. Chen, H. Ma, Z. Shen, and D. Wang, "Experiment research on the rock blasting effect with radial jet cracker," *Tunnelling and Underground Space Technology*, vol. 49, no. 1, pp. 249–252, 2015.

[10] Y. Luo and Z. Shen, "Study on orientation fracture blasting with shaped charge in rock," *Journal of University of Science and Technology Beijing: Mineral Metallurgy Materials (Eng Ed)*, vol. 13, no. 3, pp. 193–198, 2006.

[11] P. Yan, Z. Zhao, W. Lu, Y. Fan, X. Chen, and Z. Shan, "Mitigation of rock burst events by blasting techniques during deep-tunnel excavation," *Engineering Geology*, vol. 188, pp. 126–136, 2015.

[12] W. Chen, H. H. Ma, Z. W. Shen, and D. B. Wang, "High-efficiency cut blasting with shell radial shaped charge in laboratory-scale blasting," *Advanced Materials Research*, vol. 1094, pp. 445–450, 2015.

[13] Y. Wang, "Study of the dynamic fracture effect using slotted cartridge decoupling charge blasting," *International Journal of Rock Mechanics and Mining Sciences*, vol. 96, no. 1, pp. 34–46, 2017.

[14] Y. G. Du, Z. C. Zhang, and T. L. Li, "Studies on the mechanical effects produced by the v-shaped notch borehole blasting," *Explosion and Shock Waves*, vol. 11, no. 1, pp. 26–30, 1991.

[15] Z.-W. Yue, P. Qiu, X. Wang, Y. Song, and Q. Yu, "Notched-borehole cut blasting study by the method of dynamic caustics," *Journal of the China Coal Society*, vol. 41, no. 4, pp. 858–863, 2016.

[16] Z. Zheng, Y. Xu, J. Dong, Q. Zong, and L. Wang, "Hard rock deep hole cutting blasting technology in vertical shaft freezing bedrock section construction," *Journal of Vibroengineering*, vol. 17, no. 3, pp. 1105–1119, 2015.

[17] S. S. Rathore and S. Bhandari, "Controlled fracture growth by blasting while protecting damages to remaining rock," *Rock Mechanics and Rock Engineering*, vol. 40, no. 3, pp. 317–326, 2007.

[18] E. E. Wilhelm, *Multi-Point Warhead Initiation System*, United States Patent, 1989.

[19] W. Li, X. Wang, and W. Li, "The effect of annular multi-point initiation on the formation and penetration of an explosively formed penetrator," *International Journal of Impact Engineering*, vol. 37, no. 4, pp. 414–424, 2010.

[20] X. Xiao, J. H. Zhang, F. Wu, and X. L. Lei, "Numerical simulation and experimental study of double groove shaped charge detonated by two initiations," *Blasting*, vol. 32, no. 1, pp. 38–42, 2015.

[21] S. Pappu and L. E. Murr, "Hydrocode and microstructural analysis of explosively formed penetrators," *Journal of Materials Science*, vol. 37, no. 2, pp. 233–248, 2002.

[22] H. H. Yan, X. J. Li, and Z. Zhao, "Estimation of Gun overlapping probability for serial and parallel circuit," *Explosive Materials*, vol. 37, no. 2, pp. 7–9, 2008.

[23] Y. Zhang, *EFP Formation under Conditions of Detonation Wave Collision*, North University of China, 2015.

[24] B. Dunne, "Mach reflection of detonation waves in condensed high explosives. II," *Physics of Fluids*, vol. 7, no. 10, pp. 1707–1712, 1964.

[25] W. W. Wood, *Shock and Detonation Waves*, Gordon and Breach Science Publishers, 1967.

[26] B. P. Zhang, Q. M. Zhang, and F. L. Huang, *Detonation Physics*, Chapter 1, The Publishing House of Ordnance Industry, 2006.

[27] Z. Zhao, G. Tao, and C. X. Du, "Application research on JWL equation of state of detonation products," *Chinese Journal of High Pressure Physics*, vol. 23, no. 4, pp. 277–282, 2009.

[28] F. Müller, "Mach-Reflection of Detonation Waves in condensed high explosives," *Propellants, Explosives, Pyrotechnics*, vol. 3, no. 4, pp. 115–118, 1978.

[29] Y. S. Miao, X. J. Li, X. H. Wang, H. H. Yan, and C. Chen, "Munroe effect of detonation wave collision," *Explosion and Shock Waves*, vol. 37, no. 3, pp. 544–548, 2017.

[30] T. W. Shelton, J. Q. Ehrgott Jr., R. J. Moral, and M. Barbato, "Experimental and numerical investigation of the ground shock coupling factor for near-surface detonations," *Shock and Vibration*, vol. 2014, Article ID 789202, 11 pages, 2014.

[31] Z. M. Zhu, "Numerical prediction of crater blasting and bench blasting," *International Journal of Rock Mechanics and Mining Sciences*, vol. 46, no. 6, pp. 1088–1096, 2009.

[32] E. Hamdi, N. B. Romdhane, J. du Mouza, and J. M. Le Cleac'h, "Fragmentation energy in rock blasting," *Geotechnical and Geological Engineering*, vol. 26, no. 2, pp. 133–146, 2008.